Environmental Science & Technology

Article

pubs.acs.org/est

Spatiotemporal Variability of Methane Emissions at Oil and Natural Gas Operations in the Eagle Ford Basin

Tegan N. Lavoie,[†] Paul B. Shepson,[*,†,‡] Maria O. L. Cambaliza,[†,§] Brian H. Stirm,[∥] Stephen Conley,[⊥] Shobhit Mehrotra,[⊥] Ian C. Faloona,[⊥] and David Lyon[#]

[†]Department of Chemistry, [‡]Department of Earth, Atmospheric and Planetary Science and Purdue Climate Change Research Center, and [∥]School of Aviation and Transportation TechnologyPurdue University, West Lafayette, Indiana 47907, United States

[§]Department of Physics, Ateneo de Manila University, Loyola Heights, Quezon City 1108, Philippines

[⊥]Department of Land, Air and Water Resources, University of California, Davis, California 95616, United States

[#]Environmental Defense Fund, Austin, Texas 78701, United States

Supporting Information

ABSTRACT: Methane emissions from oil and gas facilities can exhibit operation-dependent temporal variability; however, this variability has yet to be fully characterized. A field campaign was conducted in June 2014 in the Eagle Ford basin, Texas, to examine spatiotemporal variability of methane emissions using four methods. Clusters of methane-emitting sources were estimated from 14 aerial surveys of two ("East" or "West") 35 × 35 km grids, two aircraft-based mass balance methods measured emissions repeatedly at five gathering facilities and three flares, and emitting equipment source-types were identified via helicopter-based infrared camera at 13 production and gathering facilities. Significant daily variability was observed in the location, number (East: 44 ± 20% relative standard deviation (RSD), N = 7; West: 37 ± 30% RSD, N = 7), and emission rates (36% of repeat measurements deviate from mean emissions by at least ±50%) of clusters of emitting sources. Emission rates of high emitters varied from 150−250 to 880−1470 kg/h and regional aggregate emissions of large sources (>15 kg/h) varied up to a factor of ∼3 between surveys. The aircraft-based mass balance results revealed comparable variability. Equipment source-type changed between surveys and alterations in operational-mode significantly influenced emissions. Results indicate that understanding temporal emission variability will promote improved mitigation strategies and additional analysis is needed to fully characterize its causes.

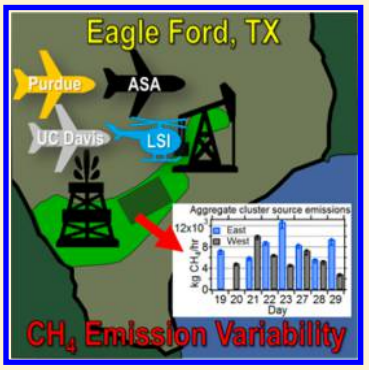

INTRODUCTION

Recent advancements in horizontal drilling and hydraulic fracturing technologies have led to a 57% increase in crude oil production and a 23% increase in natural gas gross withdrawals in the United States from 2008 to 2014.[1] The primary component of natural gas is methane (CH_4), which is a more energy efficient fuel source relative to coal or oil and releases significantly less carbon dioxide (CO_2) upon combustion.[2] However, CH_4 is also a potent greenhouse gas with 34 times the global warming potential of CO_2 on a 100-year time scale,[2] and recent studies and life cycle analyses suggest that fugitive CH_4 leaks into the atmosphere, which occur from production to distribution of natural gas, may reduce the climate benefit of the displacement of more carbon-intensive fuel sources (e.g., coal) with natural gas.[3,4] Additionally, a recent study indicated that total U.S. CH_4 emissions from all CH_4 sources increased by more than 30% from 2002 to 2014 and could contribute 30−60% of the global increase in atmospheric CH_4 concentrations.[5] Therefore, to effectively control emissions, cost-effective regulations should take into account the dynamic character of national CH_4 emissions and their sources.

To understand the current state of U.S. greenhouse gas emissions from oil and gas operations, policymakers refer to national inventories and reporting programs.[6,7] However, inventory emissions estimates often underreport emissions due to use of outdated activity and emission factors, failure to account for emissions from faulty and/or aging equipment, lack of reporting for some equipment-types and operating modes, and failure to account for skewed emissions from "super-emitters".[8−10] Independent third-party measurements often support that emissions inventories are biased low but present their own biases by only measuring emissions from one snapshot in time and, therefore, may fail to account for hourly, daily, and seasonal temporal variability of emissions. Several studies have questioned the representativeness of a single measurement as an indicator of typical facility emissions,[8,11−13] and the temporal variability of the magnitude and source of

Received: February 13, 2017
Revised: May 29, 2017
Accepted: June 15, 2017

DOI: 10.1021/acs.est.7b00814
Environ. Sci. Technol. XXXX, XXX, XXX−XXX

CH_4 emissions from oil and gas production and gathering operations has been little-studied to date.

In 2016, the Environmental Protection Agency's (EPA's) Greenhouse Gas Inventory (GHGI) reported that oil and gas systems emitted 9.8 Tg CH_4 in 2014, 70% of which originated from the production sector, which includes well production and natural gas gathering processes.[7] Recent methodological updates to the GHGI have increased annual oil- and gas-related CH_4 emissions estimates by ∼30%.[7,14] However, an independent study in the Barnett shale reported that measured emissions are still 22% higher than the updated inventory estimates.[15] To further improve national inventories, additional characterization of production and gathering emissions is needed. Oil and gas production wells typically emit CH_4 from pneumatic controllers, dehydration systems, and storage tanks, among other sources.[14] Gathering facilities, which collect natural gas from wells and pressurize the gas for downstream transport, may produce emissions from reciprocating and centrifugal compressors, dehydration and treatment systems, flares, and storage tanks.[14,16,17] Importantly, the magnitude and duration of emissions can vary depending on the operating state of equipment (i.e., operating, not-operating depressurized, not-operating pressurized modes), frequency of scheduled venting or maintenance events, occurrence of equipment malfunctions, and the age and efficiency of equipment.[14,17−19]

This study aims to understand the frequency, magnitude, and regional distribution of CH_4 emissions and how they change between periodic sampling, using data obtained from a field campaign conducted in June 2014 in the rapidly developing Eagle Ford basin. Here, we present results that assess the variability in the location, magnitude, and equipment source-type of CH_4 emissions in an area of high production in the basin using four different techniques. A series of 14 aircraft-based surveys was conducted and used to evaluate the spatiotemporal variability of CH_4 emissions. Two unique aircraft-based mass balance techniques were used to measure facility-specific CH_4 emissions to investigate emission magnitude changes over time. Furthermore, we report changes in the total count of significant sources with observed emissions between repeat visits conducted at nine oil well pads, one hydraulic fracturing operation, and three natural gas gathering stations using data obtained through helicopter-based forward-looking infrared (FLIR) camera surveys. Note that measurements from the four unique techniques were not occurring simultaneously for the same facilities, except in one case. We also evaluate the most commonly observed emission sources from 26 oil well pads, 11 gas well pads, three hydraulic fracturing operations, and one saltwater injection facility surveyed by FLIR camera. Notably, FLIR-investigated well pads in this study were a subset of 551 Eagle Ford sites surveyed as part of a different study assessing the prevalence and patterns of high emission sites in seven U.S. basins, which demonstrated the stochasticity of emissions but did not characterize their temporal variability.[20] Additionally, since FLIR videos suggested that flares were a source of fugitive emissions, three natural gas flares located at production and midstream facilities were repeatedly sampled to determine the temporal variability in CH_4 emissions. We discuss the likely reasons for spatiotemporal variability in regional CH_4 emissions from the surveys, and temporal variability of facility-specific measurements from the two aircraft-based mass balance methods and the helicopter-based FLIR videos and propose future measurement strategies which consider the effects of temporal emission variation on annual emissions.

EXPERIMENTAL METHODS

To assess the temporal variability of emissions, a combination of four techniques was employed from June 18−29, 2014 in the Eagle Ford basin, Texas, including an aircraft-based basin-wide survey approach (ASA), two aircraft-based mass-balance approaches (transect-based mass balance (TMB) and loop-based mass balance (LMB)), and helicopter-based FLIR camera surveys. In total, the study team conducted 14 regional surveys (ASA), 29 emission rate measurements (TMB, LMB), and 94 infrared camera surveys (FLIR) at 82 facilities, with repeat emission rate measurements made at 5 sites (TMB, LMB) and repeat FLIR observations made at 13 sites. This paper will primarily focus on those facilities with repeat measurements; however, results from all sites are reported in Tables S2 and S3.

Aircraft-Based Survey Approach. ASA-measured CH_4 emissions in an area of high oil and wet gas production in the Eagle Ford basin through a series of 14 4 h aerial surveys of two 35 × 35 km areas (defined in this study as the east and west sectors) over a 10 day period performed in the morning and afternoon (Table S1). Each survey flight track spanned a square area with a 2.5 km distance between each transect, flown sequentially from the downwind to upwind edge of the square flight area (Figures S17 and S18). Transects were oriented perpendicular to the prevailing wind direction (∼150°), survey altitude was 150 m above ground level (AGL), and flight speed was 250 km/h. The aircraft, a Diamond Aircraft DA42 Twin Star, was equipped with a Los Gatos Research RMT-200 fast methane analyzer to continuously measure CH_4 concentrations (1 Hz) with 1 ppb precision and 1 s response time.[21] The plane was also equipped with a GPS, radar altimeter, and high-frequency anemometer to measure altitude, attitude, position, pressure, temperature, wind velocity, and turbulence intensities.

Subsequently, measured CH_4 concentrations along the flight paths were converted to emission rate estimates and assigned to an inferred source location within the area of measurement using a Bayesian inverse solver written in Matlab (see the SI and Hirst et al.[21]). Briefly, source emission rates were estimated via a Gaussian mixture model, and atmospheric background concentration levels were represented using a spatiotemporally smooth Markov random field. The dispersion of CH_4 emissions between sources and the sampling location was represented using a Gaussian plume atmospheric eddy dispersion model including reflection terms from the ground and the atmospheric boundary layer. Initial optimization estimates of source emission rates and background concentration levels were determined using mixed $l_2 - l_1$ optimization over a discretized grid of possible ground source locations, and finally, a reversible jump Markov chain Monte Carlo (RJMCMC) inference produced estimated median values and corresponding uncertainties for the number, emission rates, and locations of ground sources.

The model infers the location of ground sources to an uncertainty of better than ±1 km (see SI), and so comparison of survey-to-survey changes in the location of emitting sources is challenging, since the uncertainty of the model would likely cause overestimation of daily variability. To overcome this limitation and allow comparison of changes in inferred source emissions over time, an aggregate analysis was performed which grouped nearby inferred source locations together, into what we will refer to as "source clusters", for sources located within a

DOI: 10.1021/acs.est.7b00814
Environ. Sci. Technol. XXXX, XXX, XXX−XXX

distance of 2 km to one another, to more than fully encompass the uncertainty of the model determination of source location. The daily emissions from each inferred source which were grouped into each cluster were summed and this sum was considered to be the total emissions per cluster per day. Mean cluster emissions for all days where the source cluster was emitting were found, and the percent deviation from mean emissions for each cluster measurement was determined for all clusters with more than 1 day of emissions (Figure S11), where $ER_{daily,clust_N}$ is the daily emission rate for some cluster N, and $ER_{avg,clust_N}$ is the average emission rate for that same cluster N, as shown in eq 1.

$$\%\text{deviation}_{daily,clust_N} = \frac{ER_{daily,clust_N} - ER_{avg,clust_N}}{ER_{avg,clust_N}} \quad (1)$$

Aircraft-Based Mass Balance Measurements of Point Sources. Sites sampled via the two aircraft-based mass balance techniques (TMB, LMB) were selected either from the helicopter surveys or from random in-flight observations of large CH_4 signals. TMB and LMB quantified total CH_4 emissions downwind of 20 unique facilities, of which five were measured more than once and seven have FLIR camera observations. Emissions from two facilities (G1, G2) were measured by both TMB and LMB, although not simultaneously, and therefore, an intermethod comparison could not be performed. However, since TMB and LMB emission rates are presented with uncertainties to 95% confidence levels (CL95), we consider measurements as significantly varying with time if they do not overlap within the uncertainty bounds, ensuring that only variability due to the true facility emissions are reported, and not variability due to differences in measurement method. Additionally, three flares at two well pads and one gathering facility were sampled multiple times by LMB to calculate changes in flare efficiency over time by determining the ratio of enhanced CH_4 to CO_2 within the sampled flare emissions (see the SI).

Flight experiments spanned 0.25−1.75 h and were conducted within the atmospheric boundary layer between 11:00 and 17:00 local time (LT) to ensure sufficient development of the convective boundary layer (CBL) and avoid changes in wind and CH_4 concentrations associated with the transition periods of CBL growth and decay (Table S2). The TMB approach was performed in Purdue's Airborne Laboratory for Atmospheric Research (ALAR, https://www.science.purdue.edu/shepson/research/BiosphereAtmosphereInteractions/alar.html, see SI), a modified twin-engine Beechcraft Duchess. The LMB approach was conducted by UC Davis and Scientific Aviation in a modified single-engine Mooney TLS aircraft (http://www.scientificaviation.com/). Both aircraft are equipped with a Picarro cavity ring-down spectroscopy (CRDS) instrument (model no. G2401-m) for high precision (TMB, 0.5 Hz; LMB, 2 Hz) measurements of CH_4, CO_2, and H_2O. The TMB aircraft is capable of high frequency (50 Hz) three-dimensional wind measurements, used in conjunction with a high precision global positioning and inertial navigation system, while the LMB aircraft is capable of high-frequency (1 Hz) horizontal wind measurements via a differential GPS system.[22] For the TMB system, in-flight and on-ground calibrations were performed daily using three National Oceanic and Atmospheric Administration (NOAA)-certified CH_4/CO_2 reference cylinders. The LMB system maintains bimonthly in-flight checks against NOAA GMD whole air sampling flasks.

Emission Quantification via Transect-Based Mass Balance Method. The CH_4 emission rate for each site measured using the TMB approach was determined according to eq 2.[8,23−25]

$$\text{emission rate}_{CH_4} = \int_0^{z_i} \int_{-x}^{+x} \Delta CH_4 \cdot U_\perp \, dx \, dz \quad (2)$$

Briefly, a series of 5−14 horizontal transects were flown at different constant altitudes at a set distance downwind (∼1−4 km) of the emitting source, creating a 2-D plane extending from near-ground to the top of the CBL. To calculate an emission rate, the perpendicular component of the mean wind ($U_\perp$) was multiplied by the CH_4 enhancement above background (ΔCH_4). ΔCH_4 was found by converting CH_4 concentrations from ppm to mol/m^3 using the molar density of air, calculated using the ideal gas law and measured data for pressure and temperature. An altitude-dependent median CH_4 background from the ends of each transect was subtracted from the measured CH_4 concentrations from each respective transect. The resulting point-by-point flux along the transects was interpolated to a two-dimensional gridded plane using the "EasyKrig 3.0" kriging software, integrated laterally across the horizontal width of the plume ($-x$ to $+x$) and vertically from the ground (0) to the top of the CBL (z_i), to a kriging resolution of 100 and 10 m, respectively, to produce a CH_4 emission rate (eq 2). Uncertainty calculations consider the uncertainties in the temperature, pressure, wind, and concentration measurements as described in the SI, and the uncertainty of the transect-based mass balance method is further discussed in Cambaliza et al.[24]

Emission Quantification via Loop-Based Mass Balance Method. The CH_4 emission rate for each site measured using the LMB approach was determined as described in Conley et al.[26] Briefly, the emitting source was circled at multiple altitudes at a distance from the source (∼1 km) optimized based on the relative time scale of horizontal mean wind advection to the large eddy turnover time of the CBL. The flight loops were flown at various altitudes randomly to mitigate the effects of any temporal trends during the sampling period, and maximum altitude was defined as the height where no discernible plume was detected for at least two loops. The path integral of the CH_4 flux (concentration fluctuation times instantaneous wind) perpendicular to the flight path was calculated for each loop, as shown in eq 3. Here

$$\oint (c' \vec{u} \cdot \hat{n}) \, dl \quad (3)$$

c' is the deviation of the CH_4 concentration from the loop mean, $u\rightharpoonup$ is the horizontal wind, $\hat{n}$ is the unit normal vector pointing outward along the loop, and l is the path circumference. The result was integrated over the depth of flight loops and equated to the source strength contained in the flight volume via Gauss' Theorem. Further details of the methodology and its verification are given in the SI and Conley et al.[26]

FLIR Camera Surveys. Simultaneously, 687 helicopter-based FLIR camera surveys, which detect CH_4, other hydrocarbons, and nonhydrocarbons (Table S3, data also presented in Lyon et al.[20]), detected emissions at 67 facilities, 13 of which were visited multiple times. Roughly 5% of visited well pads and 36% of visited gathering facilities had detectable emissions. Camera surveys were performed by Leak Surveys, Inc. (LSI) and used a FLIR GasFindIR infrared camera to identify specific equipment producing observable emissions (limit of detection (LOD): 3.6−10.8 kg/h) at facilities within

DOI: 10.1021/acs.est.7b00814
Environ. Sci. Technol. XXXX, XXX, XXX−XXX

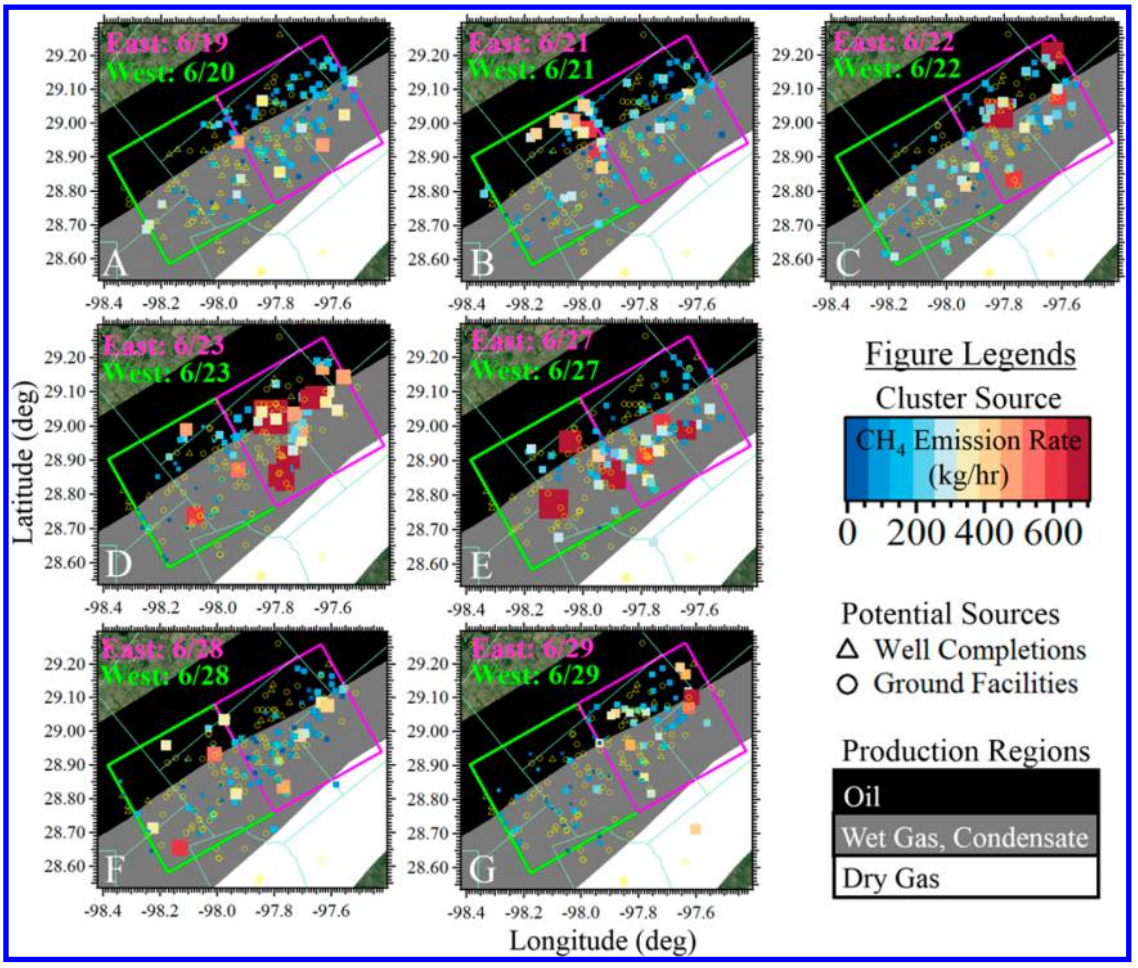

Figure 1. Spatiotemporal variability of cluster emissions. A series of 14 flight surveys of the east and west sections of the Eagle Ford basin were conducted on dates shown in the top left corner of panels A–G. Colored square markers represent cluster centers and their corresponding CH_4 emission rates (kg/h), with higher emission rates represented by warmer colors (see color scale) and larger markers. The color scale has been reduced from a maximum emission rate of 1278 to 700 kg/h for easier visualization of smaller emissions (note: only 13 of 569 data points have emission rates larger than 700 kg/h), while the size scale represents the full range of emission rates. Areas corresponding to production of oil (black), wet gas/condensate (gray), and dry gas (white) are highlighted on a map obtained from Google Earth: Landsat/Copernicus. Locations of oil and gas ground facilities (yellow circles) and well completions during the time of the study (yellow triangles) are shown for comparison.

the ASA survey region while flying at an altitude of 50 m AGL. The pilots were extensively trained in infrared gas imaging for oil and gas leak detection and instructed to locate oil- and gas-related facilities and record the site coordinates and number of visibly emitting equipment. If emissions were detectable while in flight, a video was recorded while circling the facility, focusing on the source of emissions. In total, 91 videos were recorded, and a representative FLIR video of each observed equipment source-type is provided in the supporting documents.

RESULTS AND DISCUSSION

Source Variability Based on ASA Survey Results. Sample flight paths from June 28, 2014 are provided in Figure S18 for each aircraft-based technique (ASA, LMB, TMB), during which ASA conducted a morning and afternoon survey of west and east portions of the basin, respectively, and both LMB and TMB measured emissions from two different facilities each. To minimize sampling variabilities caused by changes in atmospheric conditions, morning and afternoon ASA surveys were conducted under similar meteorological parameters (i.e., wind direction, minimal variations in CBL depth) during the same time of day (Table S1). While the CBL depth was more variable during morning flights, this has minimal influence on results due to the low transect altitude and close proximity of transects to sources.

The locations of emitting clusters per day are plotted as square markers (Figure 1), with their respective CH_4 emission rates (kg/h) depicted by size and color. The east (magenta box) and west (green box) flight tracks primarily covered areas of high oil and wet gas production, shown as black- (oil) and gray-shaded (wet gas/condensate) regions. White-shaded regions represent areas of dry gas production which were outside the survey region for this study. The composition of raw natural gas in the Eagle Ford basin varies according to reservoir and well placement, ranging from 80–95% CH_4 and 5–20% natural gas liquids, also known as condensate.[27] Condensate consists of a mixture of liquid hydrocarbons and can exist in gaseous or liquid form depending on changes in temperature and pressure.[28] Natural gas that is associated with condensate is referred to as wet gas, whereas gas produced in fields with little to no condensate is called dry gas.[28]

Within these production regions, the spatial distribution of emitting source clusters across the east and west survey grids

DOI: 10.1021/acs.est.7b00814
Environ. Sci. Technol. XXXX, XXX, XXX–XXX

(designated in Figure S18 by the magenta and green outlined regions, respectively) changed daily, with the proportion of emitting clusters in the east grid shifting from 46% (6/22) to 65% (6/27) to 55% (6/29) of the total emitting clusters for that day across both grids (Figure 1). Furthermore, of the total cluster source locations in the east (N = 146) and west (N = 148) grids, the daily number of source clusters with detectable emissions was also temporally variable by up to a factor of ~2, with an average ±1 standard deviation (σ) of 44 ± 8 in the east grid (range: 32−55), and 37 ± 10 in the west grid (range: 25−55) (Figure 2A, right axis). Additionally, 42% (east grid) and

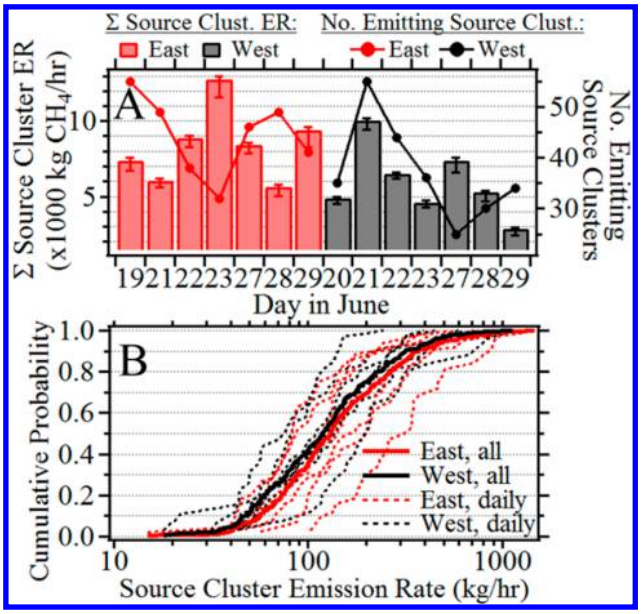

Figure 2. Daily regional CH_4 emissions variability. (A) Daily aggregate CH_4 emission rate estimates from large sources (>15 kg/h) obtained from the 14 ASA regional flight surveys for the east (red) and west (black) sectors of the basin are plotted as an average ±50% CL (left axis, bar graph with error bars). The number of emitting source clusters per flight is also shown (right axis, circles with connecting lines), where the total number of sources is 146 (east) and 148 (west). (B) Cluster emission rates from each daily flight survey from the east (red) and west (black) sectors of the basin were plotted as cumulative distribution functions. Dashed lines represent data from individual days, and solid lines represent combined data from all days within the east or west sectors.

56% (west grid) of clusters were only detected once during the survey flights. Results indicate that the location and quantity of emitting cluster sources exhibit spatiotemporal variability within the survey region.

It is clear from Figure 1 that there is substantial variability in the spatial character of emissions magnitude, e.g., comparing 6/27 with 6/29. To assess variability in cluster emissions magnitude, three analyses were performed. First, daily cluster emissions were summed to quantify temporal changes in aggregate emissions from large emission sources (LOD: > 30−40 kg/h, varies by flight). In the east sector, the average aggregate CH_4 emission rate was 8400 (±30% RSD) kg/h (N = 7), ranging from 5700^{+100}_{-600} (6/28) to 13000^{+200}_{-1200} kg/h (6/23), to 50% confidence level (CL50, Figure 2A, left axis, Table S1). In the west sector, the average aggregate CH_4 emission rate was 6000 (±40% RSD) kg/h (N = 7) and ranged from 2900^{+100}_{-400} (6/29) to $10{,}000^{+100}_{-700}$ kg/h (6/21) (CL50). Notably, the variability observed in the regional sum of cluster emissions includes compensating increases and decreases from the contributing facilities. Results indicate that the aggregate emissions from large sources are variable by up to a factor of 2.3 (east) and 3.4 (west), and the CH_4 leak rate as a percentage of average hourly total production for the east (0.9 ± 0.3%) and west (1.3 ± 0.5%) regions also varied between measurements (Table S1). Therefore, daily regional emissions variability may be significantly influenced by emission changes from large sources.

Second, there is significant variability in the distribution of emission magnitudes from high-emitting facilities in the region, defined here as the top 10% of emitting clusters, as indicated by the cumulative probability distributions (CDFs) of source cluster emission rates (Figure 2B). Data were separated by region (east: red; west: black), and plotted as individual (dashed lines) and combined days (solid lines). CDFs show that high-emitters in the east sector represent a variable range of emission rates, with 90th−100th percentile ranges of 280−450 (6/19), 230−590 (6/21), 590−1170 (6/22), 880−1470 (6/23), 330−720 (6/27), 290−450 (6/28), and 440−870 (6/29) kg/h. Similarly, high emitters in the west sector have emission rates ranging from 300−450 (6/20), 420−600 (6/21), 280−400 (6/22), 240−640 (6/23), 750−1140 (6/27), 370−590 (6/28), and 150−250 (6/29) kg/h. Markedly, clusters with only one detectable emission had emissions magnitudes similarly distributed to clusters with multiple detected emissions (see SI and Figure S12). Results indicate that there is significant variability in the magnitude of emissions from high-emitting facilities in the region.

Third, daily emission magnitude variability for individual clusters was investigated by calculating the percent deviation of each daily cluster emission rate (N = 438) from the mean emission rate for that cluster across all emitting days for the 153 clusters with two or more days of emissions (Figure 3A). Results demonstrate that 36% of repeat cluster measurements deviate by at least ±50% from the mean. Analyses were repeated using cluster distances of 3 and 4 km and trends in

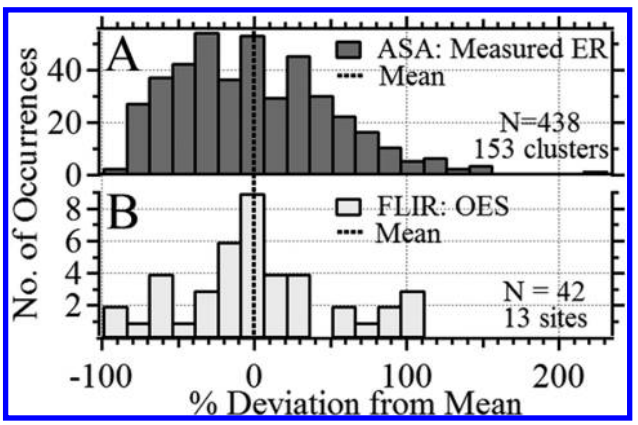

Figure 3. Temporal variability of (A) emission magnitude and (B) observed emission source counts at oil and natural gas operations. The combined percent deviations from the means for daily emission measurements and observed emission source counts at multiple facilities was plotted as a histogram with bin width of 15% deviation from the mean, using (A) ASA cluster data (438 cluster emission measurements from 153 different clusters) and (B) FLIR observed emission source (OES) counts (42 surveys at 13 different sites). Black dashed line marks 0% deviation, indicating no change in (A) emission magnitude or (B) observed emission source count over time.

DOI: 10.1021/acs.est.7b00814
Environ. Sci. Technol. XXXX, XXX, XXX−XXX

Table 1. Facility-Level Mass Balance Experiment Details and Emission Results for the TMB and LMB Methods[a]

site	latitude (deg)	longitude (deg)	FLIR	method	date	time (LT)	WS (m/s)/WDir (deg)	CH_4 ER (kg/h)
G1	28.9646	−97.7579	Y	TMB	6/21	14:50−15:20	7.0/160	17 ± 5
				LMB	6/25	12:56−13:17	6.4/128	20 ± 9
				TMB	6/26	14:09−15:09	5.6/162	740 ± 230
				LMB	6/26	15:36−15:54	4.4/157	16 ± 8
G2	28.9682	−97.8583	Y	LMB	6/26	12:14−14:08	6.0/163	46 ± 7
				TMB	6/26	15:56−16:30	4.9/165	45 ± 17
G3[b]	28.9379	−97.7975	N	TMB	6/21	14:50−15:20	7.0/160	240 ± 130
	28.9290	−97.7941		TMB	6/28	12:40−13:42	10.1/165	800 ± 200
G4	28.8699	−97.9311	N	LMB	6/23	13:22−13:45	5.6/184	87 ± 30
				LMB	6/24	12:42−12:58	2.6/235	17 ± 8
				LMB	6/25	11:30−11:54	2.4/151	93 ± 27
				LMB	6/28	11:58−12:33	10.5/166	87 ± 22
G5	29.0014	−97.7161	N	LMB	6/27	14:12−14:46	9.1/157	200 ± 90
				LMB	6/28	13:17−13:49	9.5/165	220 ± 30

[a]Summary of flight details for the TMB and LMB experiments, including site ID, coordinates (latitude and longitude), whether FLIR video was recorded for the site (Y, yes; N, no), which method performed the measurement (TMB or LMB), date and time of measurement (LT, local time), average wind speed (WS) and direction (WDir) during measurements, and calculated CH_4 emission rate (ER) in kg/h with uncertainties to CL95. [b]Represents two gathering facilities located <0.5 km away from one another, which were too close to distinguish emissions from the facilities separately.

variability were maintained (see the SI). Therefore, the ASA survey results indicate that the locations, quantities, and emissions magnitudes of emitting clusters vary considerably within the sampling region between surveys.

Quantification and Characterization of CH_4 Emissions from Oil and Gas Facilities. To reiterate, the ASA aggregate analysis clustered nearby inferred sources within a 2 km distance. Because multiple ground facilities can exist within a 2 km diameter, source attribution to one specific facility is difficult. Therefore, to understand between-measurement variability at the facility level for a few facilities, CH_4 emissions from five gathering facilities (G1−5) were measured two to four times each on different days using both aircraft-based mass balance methods, TMB and LMB, and emission rates are reported in Table 1.

Significant variability in CH_4 emissions was observed at G1, G3, and G4, while no significant variability was observed at G2 and G5. Variability in facility CH_4 emissions can be due to changes in equipment operating state and scheduled maintenance procedures, including blowdown venting into the atmosphere. During the study, FLIR camera surveys were performed over two of the measured gathering facilities (G1, G2) to determine the source of emissions. The emission rate at gathering facility G1 was measured by aircraft on four occasions and CH_4 emissions fluctuated between 17 ± 5 (15:05 LT, 6/21), 20 ± 9 (13:07 LT, 6/25), 740 ± 230 (14:39 LT, 6/26), and 16 ± 8 (15:45 LT, 6/26) kg/h (CL95). FLIR videos indicated that the quantity and type of visibly emitting equipment at G1 changed over time: (6/20) 5 tank hatches, 1 flare; (6/23 and 6/24) 1 flare; (6/25) 1 flare, 1 tank hatch; (6/26) 1 tank vent stack, 3 tank hatches, 1 flare (Table S3). The FLIR video also indicated that a blowdown event was occurring at G1 during the time of the large TMB-measured emission on 6/26 (TMB: 14:09−15:09 LT; FLIR: 14:33 LT). Blowdowns are short duration (several hours or less) discharges of emissions that occur when equipment is depressurized, and at gas processing plants, commonly have CH_4 emission rates in the magnitude of the TMB measurement of 740 kg/h (note that gathering station blowdown data will be first reported to the EPA's Greenhouse Gas Reporting Program (GHGRP) for 2016 in March 2017).[29] Therefore, our measurements support the expectation that emissions are significantly larger during blowdown events, in this case, by a factor of 46. Blowdowns can also release large quantities of other chemicals into the atmosphere, with the quantity of non-CH_4 volatile organic compounds (VOCs) varying throughout the supply chain and between basins. Therefore, improved blowdown emission controls should be considered to reduce not only CH_4 emissions but also control the release of non-CH_4 VOCs into the atmosphere.[30]

At gathering facility G2, CH_4 emission measurements were made twice on 6/26, remaining statistically constant from 46 ± 7 kg/h (13:11 LT) to 45 ± 17 kg/h (16:13 LT). The FLIR video at G2 was not recorded until 6/27 but indicated one emission from a storage tank hatch. FLIR videos are not available for G3−5. Significant emission variability occurred at G3 between the two flights that occurred 7 days apart, with emissions increasing 3-fold from 240 ± 130 (6/21) to 800 ± 200 (6/28) kg/h. At G4, three of the four measurements (6/23, 6/25, 6/28) were statistically identical (~90 ± 30 kg/h), while on 6/24 the emission rate dropped to 17 ± 8 kg/h. Emissions at G5 remained statistically unchanged from 6/27 (200 ± 90 kg/h) to 6/28 (220 ± 30 kg/h). Results indicate that, at these five gathering facilities, moment-to-moment emissions can vary or remain relatively constant due to changing operational modes and atypically large emissions can occur due to brief changes in operational conditions, as observed during the aircraft measurement of the blowdown event at G1 on 6/26.

Variability of Observed Emission Sources at Oil and Gas Facilities. To assess daily variability in the count of types of emitting equipment, repeat FLIR camera surveys were conducted at nine oil well pads (O1−9), one hydraulic fracturing operation (H1), and three gathering facilities (G1,-6,-7) belonging to 11 different operators and located within the ASA survey region. Each component-level observed emission source (OES) was counted for each day that the facility was surveyed. For surveys that detected no observable emission upon resurvey, the count was considered 0. The mean count of OESs was calculated for each site with repeat measurements, and variability was assessed by calculating the percent deviation

DOI: 10.1021/acs.est.7b00814
Environ. Sci. Technol. XXXX, XXX, XXX−XXX

of each daily OES count from the mean OES count per facility by modifying eq 1. The percent deviations from the means for each daily OES count from each of the 13 facilities were plotted as a histogram with bin width of 15% (Figure 3B). Results demonstrate that 38% of repeat OESs for each site deviated by at least ±50% from their facility-specific means, indicating that the quantity of detectable component-level emissions are also temporally variable.

To further assess the emission variability from different equipment-types, data from Figure 3B is presented in terms of specific emission source and results are reported in Table S4, where each icon represents a unique leak at a facility, with icon-shape representing equipment-type (i.e., vent, hatch, flare, etc.) and the number of icons representing the quantity of OESs. At 11 of the 13 facilities, both the equipment source-type and count of OESs varied between measurements made on different days, indicating changes in facility operating conditions. Two facilities exhibited cessation of emissions upon repeat survey 3 days later, including gathering facility G6, which initially had leaks from two storage tank hatches, and hydraulic fracturing operation H1, which had leaks from five flowback tank hatches on 6/18 and had no emissions on 6/21. Notably on 6/18, H1 was in the final stages of completion during which high volumes of used fracturing fluids are stored in temporary flowback tanks until treatment for reuse, and by 6/21 completion had ended. During the time of this study, gas wells would be legally required to flare or use green completions, but oil well completions (e.g., H1) had no control requirements. Markedly, the EPA issued New Source Performance Standard (NSPS) Subpart OOOOa in May 2016, which will now require regulation of CH_4 emissions for all oil and gas facilities that are constructed, reconstructed, or modified after September 18, 2015.[31]

While only 13 facilities had repeat FLIR camera observations, 67 sites were surveyed in total, including 25 oil well pads, 12 gas well pads, 26 gathering facilities, three hydraulic fracturing operations, and one saltwater injection facility (Table S3). To understand if equipment source-type correlates with facility-type, the fraction of leaks from tank hatches, valves, vents, flares, trucks, on-site pipelines, compressor vents, loading docks (e.g., truck loading associated with hauling of oil or condensate), and hydraulic fracturing flowback tanks was determined from the FLIR videos and sorted by facility-type (Figure 4). During each facility-level FLIR survey, all leaking components were identified, and if the same source (i.e., the tank hatch on the east-most tank) was still emitting upon repeat survey, it was only counted once. At oil and gas well pads, the most commonly observed sources of emissions were storage tank vent stacks (53%) and hatches (38%), whereas at gathering facilities, leaks were more common from storage tank hatches (62%) than vent stacks (20%). A study by Mitchell et al.[17] also reported venting from liquid storage tanks as the primary source of noncombustion emissions at gathering stations. It is expected that tanks will exhibit some venting of stored liquid vapors during normal operations and intermittent flash emission events, which occur during transfer of pressurized liquids from separators to storage tanks at atmospheric pressure and can cause temporarily increased emissions.[32] EPA compliance alert reports indicate that tank emissions controls often fail,[33] resulting in abnormal emissions from tank-related malfunctions (i.e., faulty combustor, incorrectly positioned pressure relief valves, stuck vent and/or dump valves, etc.).[17] Additionally, Mitchell et al.[17] reported that

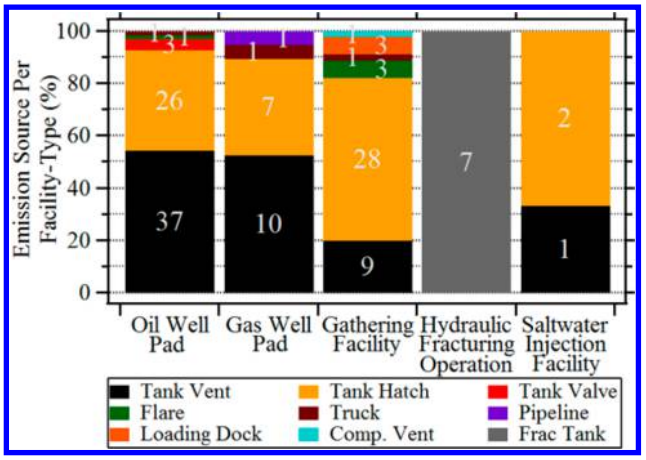

Figure 4. Percent emission source type sorted by facility type. Component-level emission sources at 26 oil well pads (N = 68 sources), 11 gas well pads (N = 19 sources), 26 gathering facilities (N = 45 sources), three hydraulic fracturing operations (N = 7 sources), and one saltwater injection facility (N = 3 sources) are grouped by facility type and shown as a percent of total emissions. Source types (i.e., tank vents, tank hatches, tanks valves, etc.) are distinguished by color according to the key. The raw number of leaking components are shown as white numbers within each color-coded component source. Abbreviations: comp vent, compressor vent; frac tank, fracturing fluid flowback tank.

gathering stations with visible liquid storage tank emissions have, on average, four times higher CH_4 emissions than facilities without liquid storage tank emissions. Therefore, improved regulations on fugitive storage tank emissions would likely be an effective component of national emissions reduction.

Flaring CH_4 Emissions. Flaring allows natural gas facilities to safely dispose of excess natural gas by combustion, converting CH_4 into CO_2 with nearly 100% efficiency when operating properly.[34] However, efficiencies can be affected by sporadic changes in operation, for instance, if flares begin sputtering or demonstrate temporary extinguishment.[34] During this study, three flares (A-C) located on an oil well pad, gathering facility (G1), and gas well pad were sampled 3, 4, and 4 times, respectively, by the LMB method and flare efficiencies were determined (Table S5). Flares were sampled for several seconds and were immediately resampled so that all repeat measurements occurred within brief timespans of 3 min (flare A), 9 min (flare B), and 16 min (flare C), to assess variability on a short time scale. Flare A (92.1 ± 0.1% RSD) and B (99.6 ± 0.3% RSD) efficiencies exhibited no significant variability, while Flare C efficiencies varied between 96.0−100% (98.8 ± 1.9% RSD), potentially due to operational fluctuations as no sputtering or extinguishment was observed. Notably, Flare A began to sputter to extinction and emit black smoke ∼5 min after sampling, which may explain its low efficiency. Results indicate that variability in flare efficiencies can occur within a short time frame. Additional measurements should be performed over longer time scales to determine if flare efficiency variability occurs during different operational periods throughout the day and across days.

Impact of Temporally Varying CH_4 Emissions on Inventory Comparisons. To enable informed policy decisions, an accurate understanding of the influence of temporal variability on annual CH_4 emissions from all sectors of the oil and gas industry is required. Multiple independent

DOI: 10.1021/acs.est.7b00814
Environ. Sci. Technol. XXXX, XXX, XXX−XXX

studies[9,17,35] have suggested that the EPA's GHGI significantly underestimates emissions. To improve certainty in such assessments, repeat emissions measurements should be performed, which consider periodic changes in emissions due to both normal and maintenance operating conditions and malfunctions. Alternatively, by sampling sufficiently large populations, single facility measurements could potentially account for temporal emissions variability, assuming that variability is expressed in the whole population data.

To improve upon current methods, several areas of future work are recommended. First, emission measurements should be performed at the same facility multiple times per day for several days, in conjunction with infrared camera surveys to elucidate the emission sources and identify the occurrence of atypical conditions. Cooperation with facility operators would further understanding of specific operating conditions during measurements. Second, this methodology could then be extended to sample multiple facilities from multiple sectors to determine typical emission rates for each operating scenario. Operator-acquired information regarding the annual percent time spent in each condition can be used to extrapolate an annual emission rate to be compared with inventories. Third, a Monte Carlo simulation, using the calculated operation-mode-dependent emission rates which account for temporal variability, can then be extrapolated to determine the national expected annual emissions per sector.

■ ASSOCIATED CONTENT

Supporting Information

The Supporting Information is available free of charge on the ACS Publications website at DOI: 10.1021/acs.est.7b00814.

Eighteen figures and five tables (PDF)
Video of FLIR camera surveys (AVI)

■ AUTHOR INFORMATION

Corresponding Author

*Phone: (765) 496-2404; fax: (765) 494-0239; e-mail: pshepson@purdue.edu.

ORCID

Tegan N. Lavoie: 0000-0002-5402-2016
Stephen Conley: 0000-0001-6753-8962

Author Contributions

The manuscript was written through contributions of all authors. All authors have given approval of the final manuscript.

Notes

The authors declare no competing financial interest.

■ ACKNOWLEDGMENTS

This work was sponsored by the Environmental Defense Fund (EDF). We thank Ramon Alvarez (EDF) for providing valuable suggestions and edits. We thank Sander Geophysics Ltd. Ottawa and the authors of ref 21 for their contributions in collecting the ASA dataset and for permitting its inclusion in this manuscript. We thank Bud McCorkle, Lisa Cantrell, Michael Mayfield, and Korey Morris from Leak Surveys, Inc., for collection of the FLIR dataset. The effort of I. Faloona was supported by the California Agricultural Experiment Station, Hatch project CA-D-LAW-2229-H.

■ ABBREVIATIONS

AGL	above ground level
ALAR	Airborne Laboratory for Atmospheric Research
ASA	aircraft-based survey approach
CBL	convective boundary layer
CH_4	methane
CO_2	carbon dioxide
CL50	50% confidence level
CL95	95% confidence level
CRDS	cavity ring-down spectroscopy
EPA	Environmental Protection Agency
FLIR	forward looking infrared
GHGI	green house gas inventory
GHGRP	Green House Gas Reporting Program
LMB	loop-based mass balance
LOD	limit of detection
LT	local time
NOAA	National Oceanic and Atmospheric Administration
OES	Observed Emission Source
RSD	relative standard deviation
SI	Supporting Information
TMB	transect-based mass balance
VOC	volatile organic compound

■ REFERENCES

(1) United States Energy Information Administration. Monthly Crude Oil and Natural Gas Production, http://www.eia.gov/petroleum/production/#ng-tab (accessed Sep 4, 2015).

(2) Myhre, G.; Shindell, D.; Bréon, F.-M.; Collins, W.; Fuglestvedt, J.; Huang, J.; Koch, D.; Lamarque, J.-F.; Lee, D.; Mendoza, B.; Nakajima, T.; Robock, A.; Stephens, G.; Takemura, T.; Zhang, H. Anthropogenic and Natural Radiative Forcing. In *Climate Change 2013: The Physical Science Basis. Contribution of Working Group I to the Fifth Assessment Report of the Intergovernmental Panel on Climate Change*; Stocker, T. F., Qin, D., Plattner, G.-K., Tignor, M., Allen, S. K., Boschung, J., Nauels, A., Xia, Y., Bex, V., Midgley, P. M., Eds.; Cambridge University Press: Cambridge, 2013; pp 659−740.

(3) Alvarez, R. A.; Pacala, S. W.; Winebrake, J. J.; Chameides, W. L.; Hamburg, S. P. Greater focus needed on methane leakage from natural gas infrastructure. *Proc. Natl. Acad. Sci. U. S. A.* **2012**, *109* (17), 6435−6440.

(4) Laurenzi, I. J.; Jersey, G. R. Life Cycle Greenhouse Gas Emissions and Freshwater Consumption of Marcellus Shale Gas. *Environ. Sci. Technol.* **2013**, *47* (9), 4896−4903.

(5) Turner, A. J.; Jacob, D. J.; Benmergui, J.; Wofsy, S. C.; Maasakkers, J. D.; Butz, A.; Hasekamp, O.; Biraud, S. C. A large increase in U.S. methane emissions over the past decade inferred from satellite data and surface observations. *Geophys. Res. Lett.* **2016**, *43* (5), 2218−2224.

(6) e-CFR: Title 40: Protection of Environment PART 98—MANDATORY GREENHOUSE GAS REPORTING. In *Electronic Code of Federal Regulations*; US Government Publishing Office, 2014.

(7) United States Environmental Protection Agency. *Inventory of U.S. Greenhouse Gas Emissions and Sinks: 1990−2014*; United States EPA: Washington, DC, 2016; p 558.

(8) Lavoie, T. N.; Shepson, P. B.; Cambaliza, M. O. L.; Stirm, B. H.; Karion, A.; Sweeney, C.; Yacovitch, T. I.; Herndon, S. C.; Lan, X.; Lyon, D. Aircraft-Based Measurements of Point Source Methane Emissions in the Barnett Shale Basin. *Environ. Sci. Technol.* **2015**, *49* (13), 7904−7913.

(9) Lyon, D. R.; Zavala-Araiza, D.; Alvarez, R. A.; Harriss, R.; Palacios, V.; Lan, X.; Talbot, R.; Lavoie, T.; Shepson, P.; Yacovitch, T. I.; Herndon, S. C.; Marchese, A. J.; Zimmerle, D.; Robinson, A. L.; Hamburg, S. P. Constructing a Spatially Resolved Methane Emission Inventory for the Barnett Shale Region. *Environ. Sci. Technol.* **2015**, *49* (13), 8147−8157.

(10) Zavala-Araiza, D.; Lyon, D.; Alvarez, R. A.; Palacios, V.; Harriss, R.; Lan, X.; Talbot, R.; Hamburg, S. P. Toward a Functional Definition

DOI: 10.1021/acs.est.7b00814
Environ. Sci. Technol. XXXX, XXX, XXX−XXX

of Methane Super-Emitters: Application to Natural Gas Production Sites. *Environ. Sci. Technol.* **2015**, *49* (13), 8167−8174.
(11) Jakober, C. A.; Mara, S. L.; Hsu, Y. K.; Herner, J. D. Mobile measurements of climate forcing agents: Application to methane emissions from landfill and natural gas compression. *J. Air Waste Manage. Assoc.* **2015**, *65* (4), 404−412.
(12) Lan, X.; Talbot, R.; Laine, P.; Torres, A. Characterizing Fugitive Methane Emissions in the Barnett Shale Area Using a Mobile Laboratory. *Environ. Sci. Technol.* **2015**, *49* (13), 8139−8146.
(13) Nathan, B. J.; Golston, L. M.; O'Brien, A. S.; Ross, K.; Harrison, W. A.; Tao, L.; Lary, D. J.; Johnson, D. R.; Covington, A. N.; Clark, N. N.; Zondlo, M. A. Near-Field Characterization of Methane Emission Variability from a Compressor Station Using a Model Aircraft. *Environ. Sci. Technol.* **2015**, *49* (13), 7896−7903.
(14) United States Environmental Protection Agency. *Inventory of U.S. Greenhouse Gas Emissions and Sinks: 1990−2013*; United States EPA: Washington, DC, 2015; p 564.
(15) Zavala-Araiza, D.; Lyon, D. R.; Alvarez, R. A.; Davis, K. J.; Harriss, R.; Herndon, S. C.; Karion, A.; Kort, E. A.; Lamb, B. K.; Lan, X.; Marchese, A. J.; Pacala, S. W.; Robinson, A. L.; Shepson, P. B.; Sweeney, C.; Talbot, R.; Townsend-Small, A.; Yacovitch, T. I.; Zimmerle, D. J.; Hamburg, S. P. Reconciling divergent estimates of oil and gas methane emissions. *Proc. Natl. Acad. Sci. U. S. A.* **2015**, *112* (51), 15597−15602.
(16) Marchese, A. J.; Vaughn, T. L.; Zimmerle, D. J.; Martinez, D. M.; Williams, L. L.; Robinson, A. L.; Mitchell, A. L.; Subramanian, R.; Tkacik, D. S.; Roscioli, J. R.; Herndon, S. C. Methane Emissions from United States Natural Gas Gathering and Processing. *Environ. Sci. Technol.* **2015**, *49* (17), 10718−10727.
(17) Mitchell, A. L.; Tkacik, D. S.; Roscioli, J. R.; Herndon, S. C.; Yacovitch, T. I.; Martinez, D. M.; Vaughn, T. L.; Williams, L. L.; Sullivan, M. R.; Floerchinger, C.; Omara, M.; Subramanian, R.; Zimmerle, D.; Marchese, A. J.; Robinson, A. L. Measurements of Methane Emissions from Natural Gas Gathering Facilities and Processing Plants: Measurement Results. *Environ. Sci. Technol.* **2015**, *49* (5), 3219−3227.
(18) Alvarez, R.; Harriss, R.; Lyon, D. Oil and Natural Gas Sector: Compressors. *Peer Rev. Responses Environ. Defense Fund* **2014**, 20.
(19) United States Environmental Protection Agency. *Lessons Learned: Directed Inspection and Maintenance at Gas Processing Plants and Booster Stations*; United States EPA, 2003; Publication No. EPA430-B-03-018.
(20) Lyon, D. R.; Alvarez, R. A.; Zavala-Araiza, D.; Brandt, A. R.; Jackson, R. B.; Hamburg, S. P. Aerial surveys of elevated hydrocarbon emissions from oil and gas production sites. *Environ. Sci. Technol.* **2016**, *50*, 4877−4886.
(21) Hirst, B.; Jonathan, P.; del Cueto, F. G.; Randell, D.; Kosut, O. Locating and quantifying gas emission sources using remotely obtained concentration data. *Atmos. Environ.* **2013**, *74*, 141−158.
(22) Conley, S. A.; Faloona, I. C.; Lenschow, D. H.; Karion, A.; Sweeney, C. A Low-Cost System for Measuring Horizontal Winds from Single-Engine Aircraft. *J. Atmos. Ocean. Technol.* **2014**, *31* (6), 1312−1320.
(23) Cambaliza, M. O. L.; Shepson, P. B.; Bogner, J.; Caulton, D. R.; Stirm, B.; Sweeney, C.; Montzka, S. A.; Gurney, K. R.; Spokas, K.; Salmon, O. E.; Lavoie, T. N.; Hendricks, A.; Mays, K.; Turnbull, J.; Miller, B. R.; Lauvaux, T.; Davis, K.; Karion, A.; Moser, B.; Miller, C.; Obermeyer, C.; Whetstone, J.; Prasad, K.; Miles, N.; Richardson, S. Quantification and source apportionment of the methane emission flux from the city of Indianapolis. *Elem. Sci. Anth.* **2015**, *3*, 000037.
(24) Cambaliza, M. O. L.; Shepson, P. B.; Caulton, D. R.; Stirm, B.; Samarov, D.; Gurney, K. R.; Turnbull, J.; Davis, K. J.; Possolo, A.; Karion, A.; Sweeney, C.; Moser, B.; Hendricks, A.; Lauvaux, T.; Mays, K.; Whetstone, J.; Huang, J.; Razlivanov, I.; Miles, N. L.; Richardson, S. J. Assessment of uncertainties of an aircraft-based mass balance approach for quantifying urban greenhouse gas emissions. *Atmos. Chem. Phys.* **2014**, *14* (17), 9029−9050.
(25) Mays, K. L.; Shepson, P. B.; Stirm, B. H.; Karion, A.; Sweeney, C.; Gurney, K. R. Aircraft-Based Measurements of the Carbon Footprint of Indianapolis. *Environ. Sci. Technol.* **2009**, *43* (20), 7816−7823.
(26) Conley, S. A.; Faloona, I. C.; Mehrotra, S.; Suard, M.; Lenschow, D. H.; Herndon, S.; Schweitzke, S. Application of Gauss's Theorem to quantify localized surface emissions from airborne measurements of wind and trace gases. *Atmos. Meas. Technol. Discuss.* **2017**, 1.
(27) Texas Commission on Environmental Quality *Final Report: Condensate Tank Oil and Gas Activities*; 2012.
(28) Troner, A. *Natural Gas Liquids in the Shale Revolution*; The James A. Baker III Institute for Public Policy of Rice University, 2013; p 98.
(29) United States Environmental Protection Agency. *Greenhouse Gas Reporting Program (GHGRP)*, https://www.epa.gov/ghgreporting (accessed: Feb 26, 2016).
(30) Texas Commission on Environmental Quality. *Air Emission Event Reporting Database*, http://www2.tceq.texas.gov/oce/eer/index.cfm?fuseaction=main.getDetails&target=212838.
(31) e-CFR: Title 40: Part 60: Subpart OOOOa—Standards of Performance for Crude Oil and Natural Gas Facilities for which Construction, Modification or Reconstruction Commenced After September 18, 2015. In *Electronic Code of Federal Regulations*; US Government Publishing Office, 2016.
(32) Brantley, H. L.; Thoma, E. D.; Eisele, A. P. Assessment of volatile organic compound and hazardous air pollutant emissions from oil and natural gas well pads using mobile remote and on-site direct measurements. *J. Air Waste Manage. Assoc.* **2015**, *65* (9), 1072−1082.
(33) United States Environmental Protection Agency. *Compliance Alert: EPA Observes Air Emissions from Controlled Storage Vessels at Onshore Oil and Natural Gas Production Facilities*; United States EPA, 2015.
(34) Caulton, D. R.; Shepson, P. B.; Cambaliza, M. O. L.; McCabe, D.; Baum, E.; Stirm, B. H. Methane Destruction Efficiency of Natural Gas Flares Associated with Shale Formation Wells. *Environ. Sci. Technol.* **2014**, *48* (16), 9548−9554.
(35) Pétron, G.; Frost, G.; Miller, B. R.; Hirsch, A. I.; Montzka, S. A.; Karion, A.; Trainer, M.; Sweeney, C.; Andrews, A. E.; Miller, L.; Kofler, J.; Bar-Ilan, A.; Dlugokencky, E. J.; Patrick, L.; Moore, C. T.; Ryerson, T. B.; Siso, C.; Kolodzey, W.; Lang, P. M.; Conway, T.; Novelli, P.; Masarie, K.; Hall, B.; Guenther, D.; Kitzis, D.; Miller, J.; Welsh, D.; Wolfe, D.; Neff, W.; Tans, P. Hydrocarbon emissions characterization in the Colorado Front Range: A pilot study. *J. Geophys. Res.: Atmos.* **2012**, *117* (D4), D04304.

DOI: 10.1021/acs.est.7b00814
Environ. Sci. Technol. XXXX, XXX, XXX−XXX